Geomechanics and Engineering, *Vol. 15, No. 6 (2018) 1161-1171*
DOI: https://doi.org/10.12989/gae.2018.15.6.1161

The establishment of IB-SEM numerical method and verification of fluid-solid interaction

Jing Wang[1a], Shu-cai Li[1b], Xuerui Mao[2c], Li-ping Li[*1], Shao-shuai Shi[1d] and Zong-qing Zhou[1e]

[1]*Geotechnical and Structural Engineering Research Center, Shandong University, Jinan 250061, Shandong, China*
[2]*State Key Lab of Subtropical Building Science, South China University Of Technology, Guangzhou 510005, Guangdong, China*

(Received December 26, 2017, Revised March 9, 2018, Accepted April 7, 2018)

Abstract. The interaction between particles and fluid was investigated by IB-SEM numerical method which is a combination of combing the spectral/hp element method and the rigid immersed boundary method. The accuracy of this numerical method was verified based on the computed results with the traditional body-fitted mesh in numerical simulation of the flow through the cylinder. Then the governing equations of particles motion and contact in fluid are constructed. The movement of the particles and the interaction between the fluid and the particles are investigated. This method avoided the problem of low computational efficiency and error caused by the re-division of the grid when the solids moved. Finally, the movement simulation of multi particles in the fluid was carried out, which can provide a completely new numerical simulation method.

Keywords: the spectral/hp element method; the rigid immersed boundary method; flow through the cylinder; movement simulation of multi particles

1. Introduction

Simulations of the interaction between particle and fluid with high accuracy are difficult (Niroumand *et al.* 2016, Hu *et al.* 2001). The major challenge is how to deal with the boundary between particles and fluid (Zhao *et al.* 2016, Weirich *et al*. 2014, Abbas 2014). The ALE method (arbitrary-Lagrangian-Eulerian) needs to regenerate the grid, a large amount of computing resources are consumed and the accuracy of calculation is relatively low. The LBM method (lattice Boltzmann method) uses the regular boundary points to approximate the moving boundary (Ladd 1994). The simulated boundary is not coincident with the physical boundary, and sometimes leads to the calculation of the fluid solid interaction force.

The IB method (immersed boundary method) (Coulonius and Taira 2008, Yang and Stem 2015). This method used the Cartesian grid to compute the fluid-solid coupling. The immersed boundary method is not only a mathematical modeling method, but also a numerical discretization method. Its core idea is the numerical simulation of the boundary of the object.

The immersed boundary method is focus on the elastic boundary. But the research of water inrush through filling structure need the rigid boundary. At first, the solid boundary problem was solved by the rigid spring, which was connected with the boundary element to be modeled, and the elastic boundary was reached to a rigid limit to satisfy the condition of no slip boundary condition. But the computation efficiency of this method was very low. The classical model proposed by Peskin couldn't be used to directly solve the rigid problems (Peskin 1977). Virtual Boundary is also called Feed forcing method. It's one of the most effective rigid immersed boundary method which restart from the core idea of the immersed boundary method numerical simulation of object boundary, combined with other concepts, reconstruct the source function. The fluid-solid interaction used in this paper is also based on this method.

Semtex is a direct numerical simulation CFD code that uses the spectral element method as the underlying discretization. Semtex and immersed boundary method are combined to establish the IB-SEM system. Then the system is used to study the fluid-solid interaction.

2. The IB-SEM numerical system

2.1 The spectral method

The spectral methods are a class of techniques used in applied mathematics and scientific computing to numerically solve certain differential equations, often involving the use of the Fast Fourier Transform. The idea is to write the solution of the differential equation as a sum of

∗Corresponding author, Professor
E-mail: yuliyangfan@163.com
[a]Ph.D.
E-mail: wjingsdu@163.com
[b]Professor
E-mail: lishucai@sdu.edu.cn
[c]Associate Professor
E-mail: Xuerui.Mao@nottingham.ac.uk
[d]Lecture
E-mail: shishaoshuai@sdu.edu.cn
[e]Lecture
E-mail: zongqing.zhou@sdu.edu.cn

ISSN: 2005-307X (Print), 2092-6219 (Online)

certain "basis functions" (for example, as a Fourier series which is a sum of sinusoids) and then to choose the coefficients in the sum in order to satisfy the differential equation as well as possible.

The single expansion of the function which used in the classic spectral method is

$$u(x) \approx u^{\delta}(x) = \sum_{i=0}^{n} \phi_i(x) u_i \quad (1)$$

Where, $\phi_i(x)$ are the trial functions. The approximated function in expanded form $u^{\delta}(x)$ is substituted into the differential equations to compute the unknown coefficients u_i.

There are different schemes for minimizing the residual of the discretized governing equations. So the spectral method can be broadly classified into two categories: the pseudo-spectral or collocation methods and the modal or Galerkin methods.

The collocation method is a method for the numerical solution of ordinary differential equations, partial differential equations and integral equations. The idea is to choose a finite-dimensional space of candidate solutions (usually polynomials up to a certain degree) and a number of points in the domain (called collocation points), and to select that solution which satisfies the given equation at the collocation points.

The Galerkin method is used to convert a continuous problem in the area of numerical analysis. In principle, it first selects the basic functions and overlays them. Then the results in the domain and weighted integrals of the boundary satisfy the original equation. At last, a set of linear algebraic equations can be obtained and natural boundary conditions can be automatically satisfied. This method simplified the problem of solving the differential equations to solve the problem of linear equations. But as a trial function of the basis function, this method can only obtain an approximate solution in the domain which only the weighted average satisfied the original equation and not satisfied at every point.

2.2 Introduction of Semtex

2.2.1 Feature of Semtex

Orthogonal polynomial-based shape functions Spectral accuracy is achieved by using tensor-product Lagrange interpolants within each element, where the nodes of these shape functions are placed at the zeros of Legendre polynomials mapped from the canonical domain [−1, 1]×[−1, 1] to each element.

Gauss-Lobatto quadrature Efficiency (particularly in iterative methods) is achieved by using Gauss-Lobatto quadrature for evaluating elemental integrals: the quadrature points reside at the nodal points, which enables fast tensor-product techniques to be used for iterative matrix solution methods. Gauss-Lobatto quadrature delivers diagonal mass matrices.

Static condensation direct matrix solutions are sped up by using static condensation coupled with bandwidth reduction algorithms to reduce storage requirements for assembled system matrices.

While the numerical method is very accurate and efficient, it also has the advantage that complex geometries can be accommodated by employing unstructured meshes. The vertices of spectral elements meshes can be produced using finite-element mesh generation procedures.

Time integration employs a backwards-time differencing scheme described by Karniadakis *et al*. (1991), more recently classified as a velocity-correction method by Guermond and Shen (2003). One can select first, second, or third-order time integration, but second order is usually a reasonable compromise, and is the default scheme. Equal-order interpolation is used for velocity and pressure (see Guermond *et al*. 2006).

2.2.2 The implementation

The top level of the code is written in C++, with calls to C and FORTRAN library routines, e.g., BLAS and LAPACK. The original implementation for two-dimensional Cartesian geometries was extended to three dimensions using Fourier expansion functions for spatially-periodic directions in Cartesian and cylindrical spaces. Concurrent execution is supported, using MPI as the basis for inter processor communications, and the code has been ported to DEC, NEC, Fujitsu, Compaq, SGI, Apple and Linux multiprocessor machines. Basically it ought to work with little trouble on any contemporary UNIX system.

Various code extensions are not part of the base distribution. These include dynamic and non-dynamic LES (Blackburn and Schmidt 2003), simple power-law type non-Newtonian theologies (Rudman and Blackburn 2006), scalar transport (Blackburn 2001, 2002a), buoyancy via the Bossiness approximation, accelerating frame of reference coupling for aero elasticity (Blackburn and Henderson 1996, 1999, Blackburn *et al*. 2001, Blackburn 2003), solution of steady-state flows via Newton-Raphson iteration (Blackburn 2002b), linear stability analysis (Blackburn 2002b, Blackburn and Lopez 2003a, b, Blackburn *et al.* 2005, Sherwin and Blackburn 2005, Elston *et al*. 2006) respectively.

Semtex is a family of spectral element simulation codes. The spectral element method is a high-order finite element technique that combines the geometric flexibility of finite elements with the high accuracy of spectral methods. The method was pioneered in the mid 1980's by Anthony Patera at MIT (Patera 1984, Korczak and Patera 1986). Semtex uses parametrically mapped quadrilateral elements, the classic GLL 'nodal' shape function basis, and continuous Galerkin projection. Algorithmically the code is similar to Ron Henderson's Prism (Henderson and Karniadakis 1995, Karniadakis and Henderson 1998, Henderson 1999), but with some differences in design, and lacking mortar element capability. A notable extension is that Semtex can solve problems in cylindrical as well as Cartesian coordinate systems (Blackburn and Sherwin 2004).

2.3 The rigid immersed boundary method

The main idea of this method is that the fluid velocity equal to the speed of the object boundary through exerting a

force on the fluid near the boundary in the non-slip boundary condition.

The incompressible viscous fluid flow is governed by the N-S equations and the continuity equation

$$\rho_0\left(\frac{\partial u}{\partial t}+u\cdot\nabla u\right)=-\nabla p+\mu\nabla^2 u+f \tag{2}$$

$$\nabla\cdot u=0 \tag{3}$$

Where $u=(u,v)$ is the velocity vector, p is the pressure, ρ_0 is the fluid density, μ is the dynamic viscosity, and $f=(f_x,f_y)$ is the momentum forcing applied to enforce the no-slip boundary condition along the IB.

The governing equations for a filament is written in a Lagrangian form. The motion equations are

$$\frac{\partial^2 X}{\partial t^2}=\frac{\partial}{\partial s}\left(T\frac{\partial X}{\partial s}\right)-\frac{\partial^2}{\partial s^2}\left(\gamma\frac{\partial^2 X}{\partial s^2}\right)+\rho_1 g-F+F_c \tag{4}$$

The interaction force between the fluid and the IB can be calculated by the feedback law

$$F=\alpha\int_0^t(U_{ib}-U)dt'+\beta(U_{ib}-U) \tag{5}$$

Where α and β are large negative free constants, U_{ib} is the fluid velocity obtained by interpolation at the IB, and U is the velocity of the solid expressed by $U=dX/dt$. Eq. (2) implies that the adjacent fluid points are linked with the IB by a set of identical stiff springs with damping. No-slip boundary condition can be satisfied by the above equation. In the expression, the α will continue to grow as the speed difference increases to eliminate the difference. β can be understood as the resistance to the surface of the object, the resistance will affect the elimination of the speed difference. For different situations, α and β will have a corresponding coefficient value range. In this range, the value of the two coefficients has little effect on the calculation results.

In the virtual boundary method, the limiting expression for time step is

$$\Delta t<\frac{-\beta-\sqrt{(-\beta^2-2\alpha k)}}{\alpha} \tag{6}$$

2.4 Discretization of the NS equations

Discretization of the Navier-Stokes equations is a reformulation of the equations in such a way that they can be applied to computational fluid dynamics.

The equation was divided by the density and density was absorbed into the body force term.

$$\frac{\partial u_i}{\partial t}+\frac{\partial u_i\,\partial u_j}{\partial x_i}=-\frac{\partial P}{\partial x_i}+\nu\frac{\partial^2 u_i}{\partial x_i\,\partial x_j}+f_i \tag{7}$$

The equation is integrated over the control volume of a computational cell.

$$\iiint_V\left[\frac{\partial u_i}{\partial t}+\frac{\partial u_i\,\partial u_j}{\partial x_i}\right]dV$$

$$=\iiint_V\left[-\frac{\partial P}{\partial x_i}+\nu\frac{\partial^2 u_i}{\partial x_i\,\partial x_j}+f_i\right]dV \tag{8}$$

The time-dependent term and the body force term are assumed constant over the volume of the cell. The divergence theorem is applied to the advection, pressure gradient, and diffusion terms.

$$\begin{aligned}&\frac{\partial u_i}{\partial t}V+\iint_A u_i u_i n_j\,dA\\&=-\iint_A Pn_i dA+\iint_A\frac{\partial u_i}{\partial x_i}n_j dA+f_i V\end{aligned} \tag{9}$$

Where n is the normal of the surface of the control volume and V is the volume. If the control volume is a polyhedron and values are assumed constant over each face, the area integrals can be written as summations over each face.

$$\begin{aligned}&\frac{\partial u_i}{\partial t}V+\sum_{nbr}(u_i u_i n_j A)_{nbr}\\&=-\sum_{nbr}(Pn_i A)_{nbr}+\sum_{nbr}\left(\nu\frac{\partial u_i}{\partial x_j}n_j A\right)_{nbr}+f_i V\end{aligned} \tag{10}$$

Where, the subscript *nbr* denotes the value at any given face.

For a two-dimensional Cartesian grid, the equation can be expanded to

$$\begin{aligned}&\frac{\partial u_i}{\partial t}\Delta x\Delta y-(u_i u\Delta y)_\omega+(u_i u\Delta y)_e-(u_i\nu\Delta x)_S\\&+(u_i\nu\Delta x)_n=-(Pn_i\Delta y)_\omega-(Pn_i\Delta y)_e\\&-(Pn_i\Delta x)_S-(Pn_i\Delta x)_n-\left(\nu\frac{\partial u_i}{\partial x}\Delta y\right)_\omega\\&+\left(\nu\frac{\partial u_i}{\partial x}\Delta y\right)_e-\left(\nu\frac{\partial u_i}{\partial y}\Delta x\right)_S+\left(\nu\frac{\partial u_i}{\partial y}\Delta x\right)_n+f_i\end{aligned} \tag{11}$$

2.5 Simulation of IB-SEM system

The IB-SEM system was established based on the Spectral element method Semtex and the rigid immersed boundary method. The work-flow of the IB-SEM system was shown in Fig. 1.

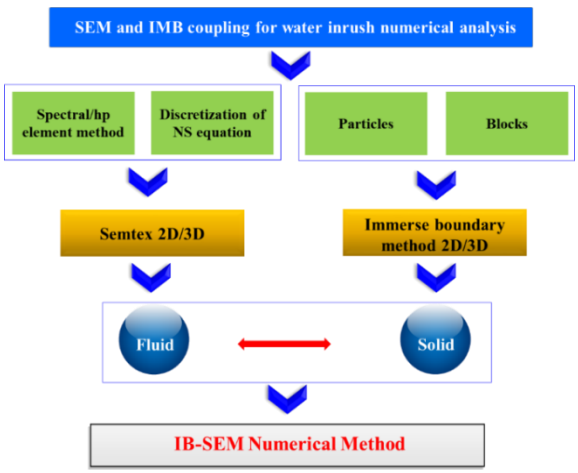

Fig. 1 The work-flow of IB-SEM system

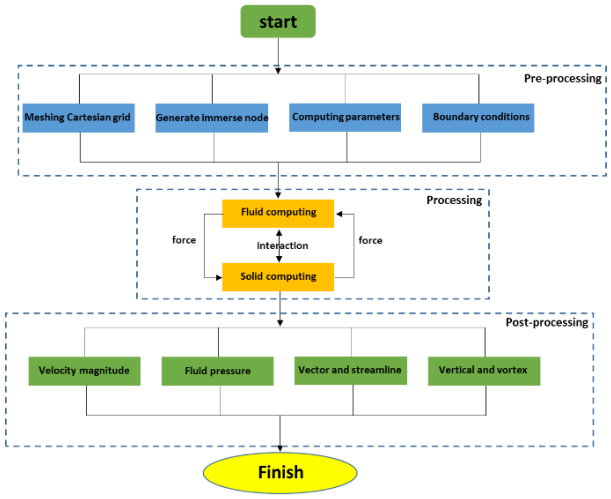

Fig. 2 The simulation process of IB-SEM system

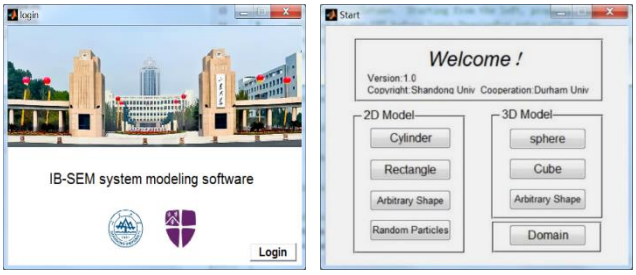

Fig. 3 IB-SEM system modeling software

This system is used to simulate the interaction of the solid and fluid which are shown in Fig. 2.

First, in the pre-processing, the modeling software of the IB-SEM system was established. This software was used to realize two dimensional and three dimensional immerse boundary modeling and the elements and nodes of fluid domain generating (see Fig. 3).

In the processing, Fig. 4 shows the interaction of solid and fluid in the IB-SEM system. Where, Ω_f is the fluid zone, Ω_s is the solid zone, f is the momentum forcing applied to enforce the no-slip boundary condition along the immerse boundary, P is the water pressure, τ is the viscous force, h_x is the length of each element, h_y is the width of each length, the red points are immersed points and the blue pints are fluid nodes.

The simulation process of the system is shown in Fig. 4.

In the post-processing, we used Tecplot 360 EX 2015 *R*2 software to display and analysis the simulation results.

3. Flow around the fixed particle

When there are not the complex or moving solid boundary in the simulation, the accuracy of the traditional finite element grid is very good. So in order to verify the accuracy of the immersed boundary method, the particle was fixed and investigated the two dimensional flow around it, and then comparing with the result based on the fitted gird in this section.

The numerical model integrates the two-dimensional,

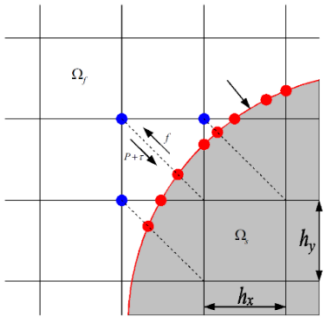

Fig. 4 Solid immersed in a Cartesian grid

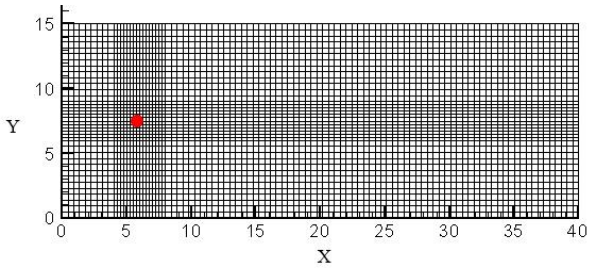

Fig. 5 Spectral elements in the overall computational domain

time-dependent, incompressible, Navier-Stokes equations, continuity equations and dimensionless by the diameter of the cylinder and the free-stream velocity. All lengths are expressed in terms of the diameter of the cylinder, The Reynolds number is 150. The center of the immerse boundary cylinder is (5, 5) in the Cartesian coordinate system, and the diameter is 1. The length of the computational domains is 25, and the width is 10.The inflow is located at x=0 and the outflow is located at x=25. The far-field boundaries are located at y=0 and y=10. The coordinates of monitoring points is (6.5, 6). Free stream boundary conditions with $u = 1.0$ and $v = 0$ are applied into the inflow boundary.

The 2D computational domain is decomposed into 1775 spectral elements and 11111 nodes. The spectral elements employing piecewise continuous nodal-based polynomial expansions within mapped-quadrilateral elemental subdomains are adopted for two-dimensional spatial discretization. In each of element, piecewise continuous nodal-based polynomial expansions with order P are applied. In this numerical the polynomial order P is 6. The number of points defining the cylinder is 1401. The domain and the computational grid are shown in Fig. 5.

The feedback forcing coefficients was set to $\alpha = -400000$ and $\beta = -600$. The Δt was valued at 0.001 in our simulation.

As shown in Fig. 6, in the process of flow simulation, due to the large Reynolds number, the particle vibration, which produces the vortex. And as the flow continues, the frequency of the oscillation period tends to be stable.

The following table lists the particle of the immerse boundary results comparing with previous traditional cylinder flow numerical simulation studies. On Table 1, the $Re = 150$, the C_l' means the lift coefficients, C_d means the drag coefficient, C_d' means the amplitude of the fluctuating part of the drag and S_t means the Strouhal

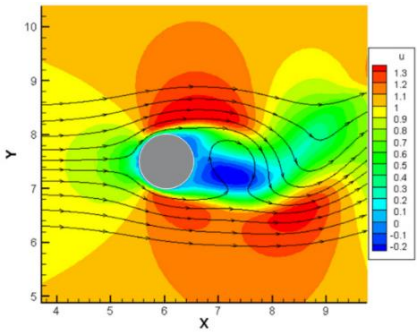

(a) Streamline

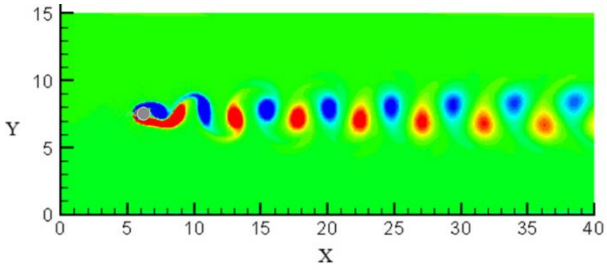

(b) Vortex flow around a particle

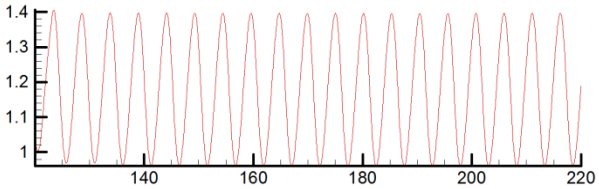

(c) Lift drag coefficient

Fig. 6 Numerical simulation of flow through the particle (*Re*=150)

number. The calculation method of above parameters were shown in below:

(1) The lift coefficient C_l' is defined by

$$C_l' = \frac{L}{qS} = \frac{L}{\frac{1}{2}\rho u^2 S} = \frac{2L}{\rho u^2 S} \tag{12}$$

Where, L is the lift force, q is the fluid dynamic pressure, S is the relevant plan area, ρ is the fluid density and u is the flow speed.

(2) The drag coefficient is defined as

$$C_d = \frac{2F_d}{\rho u^2 A} = \frac{8F_d}{\rho u^2 \pi D^2} \tag{13}$$

Where, F_d is the drag force, the F_d is defined as

$$F_d = \int_\Gamma f_x^B d\Gamma \tag{14}$$

$$F_{dx} = \tau_x + p_x \tag{15}$$

$$F_{dy} = \tau_y + p_y \tag{16}$$

ρ is the mass density of the fluid, u is the mean free stream velocity. A is the reference area

$$A = \pi D^2/4 \tag{17}$$

Table 1 Flow past a cylinder at Re=150

Studies	C_l'	C_d	C_d'	S_t
Williamson (1988)				0.184
Zhang *et al*. (1995)	0.403	1.410	0.030	0.192
Liu *et al*. (1998)	0.530	1.334	0.026	0.182
Kumar and Mittal (2012)	0.518	1.313	0.026	0.182
Present results	0.526	1.335	0.026	0.183

(3) The Strouhal number (S_t) is a dimensionless number describing oscillating flow mechanisms.

The Strouhal number is often given as

$$S_t = \frac{fL}{U} \tag{18}$$

Where, f is the frequency of vortex shedding, L is the characteristic length (the diameter of circle), and U is the flow velocity.

By comparing the results (see Table 1), we can see that the results were basically consistent, and the fluid structure coupling phenomenon was the same. So the method is feasible.

Numerical simulation of flow around a particle under different Reynolds number is carried out. The flow streamlines are as follows (black particles).

In the *Re*<1, the stokes-Oseen solutions can be used. Except that, finding the analytical solutions became an impossible work and the analysis needed to depend on the numerical and experimental solutions.

From the simulation in Fig. 7, we can see that when the Reynolds number of the flows was small enough (*Re*<1), the inertia forces were negligible over most of the flow field, the streamlines appeared symmetrically from front to rear. When the Reynolds number exceeded 1, the symmetry was lost. As the Reynolds increased from 20 to 50, a pair of upper and lower vortices was generated within the wake of the cylinder. After the Reynolds exceeded 50, the vortex region expanded and increased in length.

4. Motion of the single particle in the flow

4.1 Governing equations for particle motion

(1) Calculation the vector force of the particle

The velocity vector around of the particle can be decomposed in the Cartesian coordinates as u_x , u_y and u_z, or as a surface-normal component u_n, a stream wise component u_m and a span wise component u_z

$$u = u_x i + u_y j + u_z k = u_n n + u_m m + u_z k \tag{19}$$

Where *i*, *j*, *k*, *n* and *m* are units in the *x*, *y*, *z*, outward surface-normal and stream wise directions, respectively. *n* and *m* can be decomposed as $n = n_x i + n_y j$ and $m = m_x i + m_y j$, where $m_x = n_y$ and $m_y = n_x$. Correspondingly there are $u_n = u_x n_x + u_y n_y$, $u_m = u_x m_x + u_y m_y$, $u_x = u_m m_x + u_n n_x$ and $u_y = u_m m_y + u_n n_y$. In this work, it is assumed that the controlled boundary is a concave and closed surface (curve) and u_x,

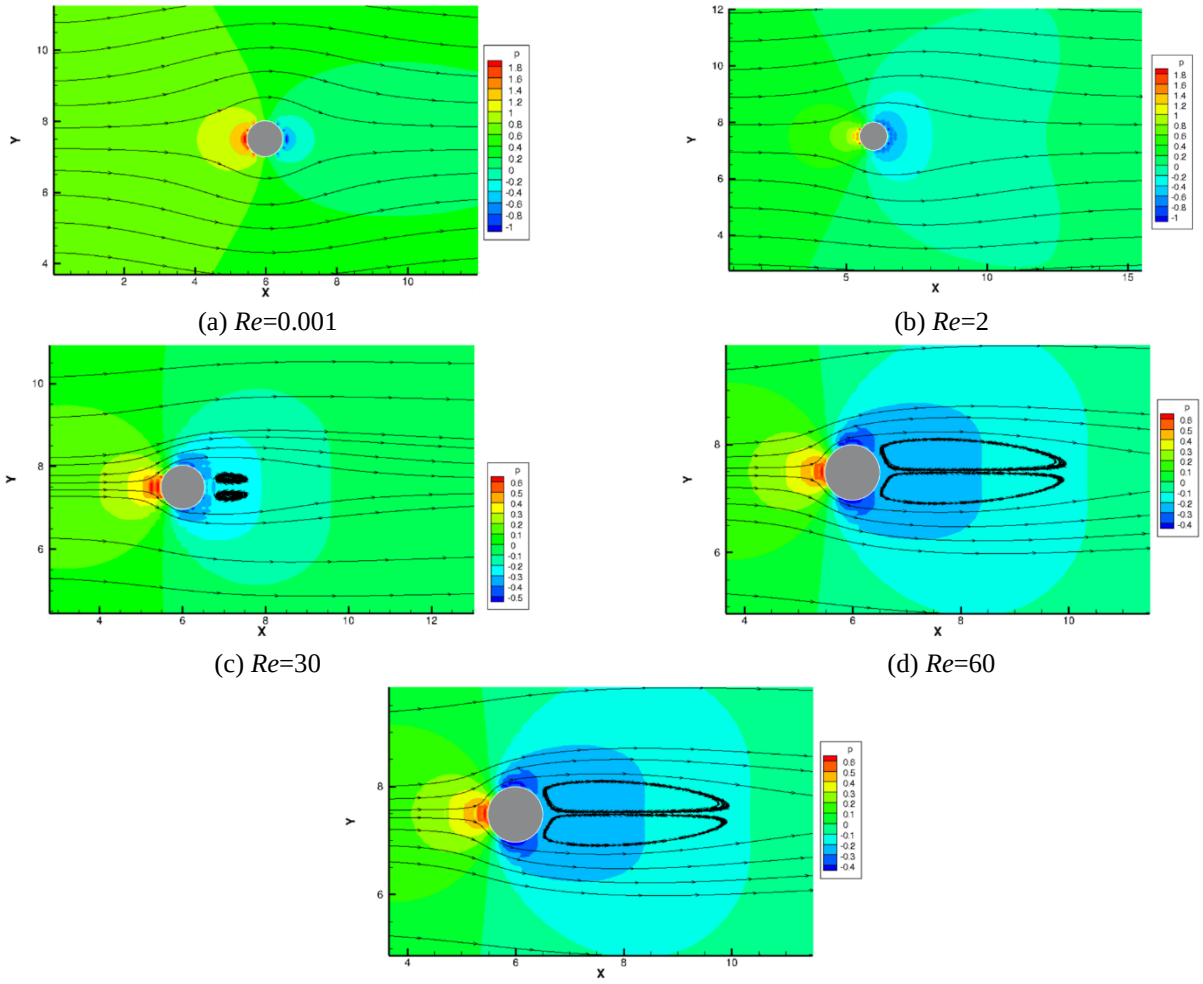

(a) *Re*=0.001 (b) *Re*=2

(c) *Re*=30 (d) *Re*=60

(e) *Re*=301

Fig. 7 Numerical simulation of flow around particle in different Reynolds numbers

u_y, m_x and m_y are differentiable.

The force acting on the surface of the solid body C can be written as

$$f = \int_C (pn - \tau \cdot n + uu_n)dS \tag{20}$$

Where, the three terms integrated represent pressure, viscous and thrust terms. τ is the viscous shear stress and

$$\tau \cdot n = Re^{-1}\begin{bmatrix} 2\partial_x u_x & \partial_y u_x + \partial_x u_y \\ \partial_y u_x + \partial_x u_y & 2\partial_y u_y \end{bmatrix} \cdot \begin{bmatrix} n_x \\ n_y \end{bmatrix} \tag{21}$$

The force of viscous force in X direction and Y direction are respectively

$$\tau_x = \mathrm{Re}^{-1}(2\partial_x u_x * n_x + \partial_y u_x * n_y + \partial_x u_y * n_y) \tag{22}$$

$$\tau_y = \mathrm{Re}^{-1}(2\partial_y u_y * n_y + \partial_y u_x * n_x + \partial_x u_y * n_x) \tag{23}$$

(2) The governing equations for particle motion

The calculation of the water pressure is

$$p_x = p * n_x \tag{24}$$

$$p_y = p * n_y \tag{25}$$

The motion of the particle include the translation and the rotation respectively. The motion of the particles can be calculated through the Newton's equation. X direction and Y direction resultant force are respectively

$$F_x = v_x + p_x \tag{26}$$

$$F_y = v_y + p_y + mg \tag{27}$$

Because the block is seemed as a series of points in the immersed boundary method, the motion of the block is divided into translation and rotation.

In the translation, all the points have the same accelerate and velocity.

$$a_x = \frac{F_x}{m} \tag{28}$$

$$a_y = \frac{F_y}{m} \tag{29}$$

$$V_x = V_0 + a_x t \tag{30}$$

$$V_y = V_0 + a_y t \tag{31}$$

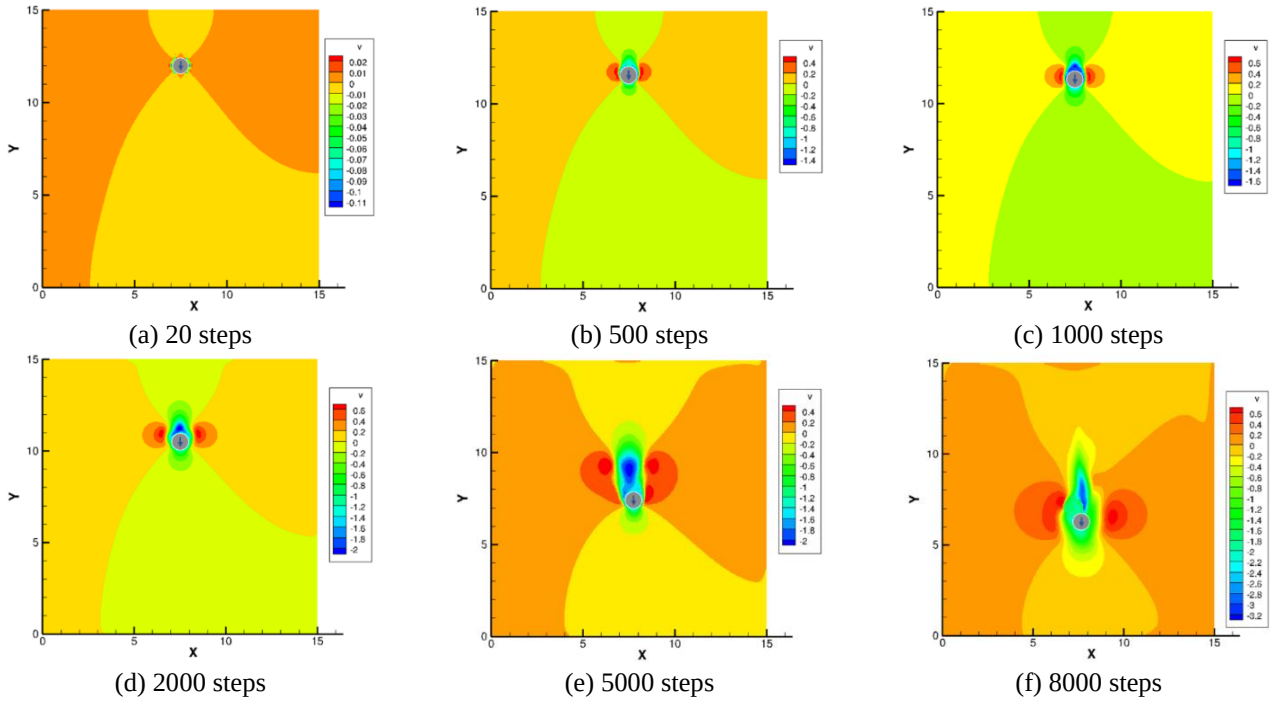

(a) 20 steps (b) 500 steps (c) 1000 steps

(d) 2000 steps (e) 5000 steps (f) 8000 steps

Fig. 8 The velocity of the particle sedimentation

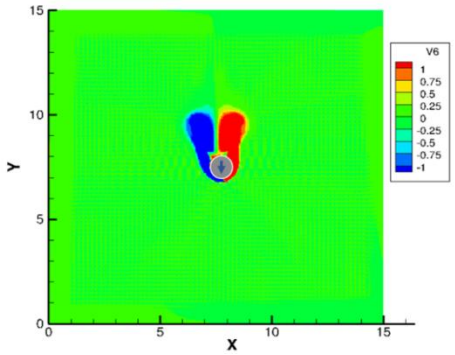

Fig. 9 The vortex structures in the particle sedimentation progress

4.2 Numerical simulation of the single particle motion

(1) The sedimentation of the particle

First, the velocity of flow is 0, which is the study of the interaction between the sedimentation of particles and the flow field. At different steps, the velocity of particles and the effect of the vortex are shown in Figs. 8 and 9.

It can be found that the surface of the particles is significantly affected by the pressure. The effect of fluid motion and the governing equation of motion of the fluid are explained by the symmetry of the flow line. In the process of settling of particles, the wake flow is gradually produced and developed. The greater velocity of the water body near the particle, the more vortex appears. This is basically consistent with the results of previous experiments (see Figs. 8 and 9).

Then on the left side of the imported u=1, in the case of the flow of particles, the trajectory of the movement and the flow char from left to right is as follows (Fig. 10):

Through the study we found that the particle trajectory is parabolic shape. And with the continuous movement of the particles, the vortex effect becomes more and more obvious. The position of the vortex is mainly concentrated in the upper left and the upper right of the particle.

In comparison with the traditional finite element method, the mesh does not need to be rebuilt when the solid is moved by the fluid, which greatly improves the computational efficiency and reduces the error.

The traditional particle discrete element method can only simulate fluid solid coupling through interaction between particles, which cannot describe the flow field accurately and effectively. Rigid boundary immersion method solve the above problems, more in line with the actual.

5. Collision model for the numerical simulation

In the numerical simulation, the overlap of the particles may happen. The repulsive force model was established to avoid the overlap. It can also prevent the particles from getting too close which may lead to the unavoidable numerical truncation errors. The collisions include the particle-particle collisions and the particle-wall collisions respectively.

5.1 Particle-particle collisions

The collision model was established to prevent the particles from interpenetration each other. A repulsive force was proposed by Glowinski et.al which can prevent the particles from getting too close. The repulsive force was determined as

$$F_{i,j}^{p} = \tag{32}$$

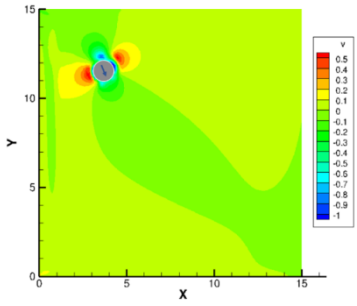

(1a) The velocity of particles in the 1000 step V cloud image

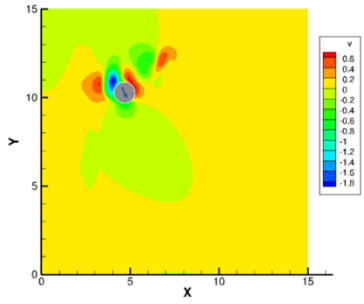

(2a) The velocity of particles in the 3000 step V cloud image

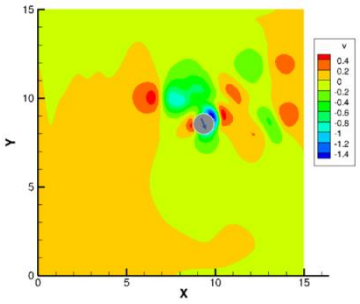

(3a) The velocity of particles in the 10000 step V cloud image

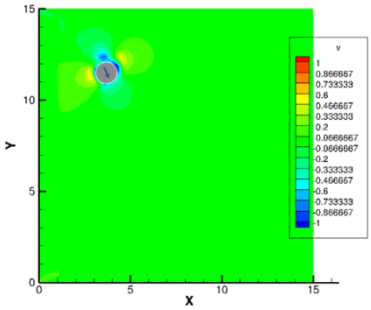

(1b) Vortex chart of 1000 steps

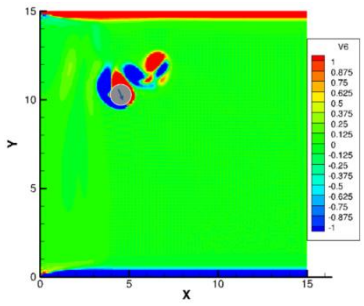

(2b) Vortex chart of 3000 steps

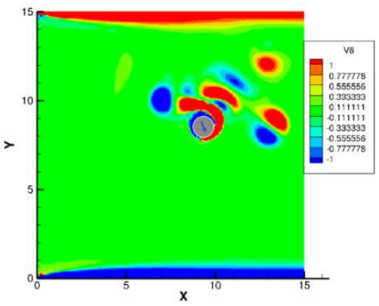

(3b) Vortex chart of 10000 steps

Fig. 10 The progress of the particle motion (u=1)

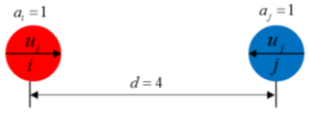

Fig. 11 The diagram of collision of two particles

$$\begin{cases} 0 & d_{i,j} > R_i + R_j + \rho \\ \frac{1}{\varepsilon_p}(X_i - X_j)(R_i + R_j - d_{i,j}) & R_i + R_j \le d_{i,j} < R_i + R_j + \rho \\ \frac{1}{\varepsilon_p'}(X_i - X_j)(R_i + R_j + \rho - d_{i,j})^2 & d_{i,j} < R_i + R_j \end{cases}$$

Where, d_{ij} is the distance between the i particle and the j particle. R_i and R_j are the radius of the i and j particle. The ε_p and ε_p' are small positive stiffness parameters. The ρ is the range of the repulsion force. It was taken $\rho \simeq h_\Omega$ (h_Ω is the space discretization step used for approximating the velocity).

The h_Ω can be adjusted so that the finite element approximation can resolve the boundary and shear layers occurring in the flow. The ρ can be taken of the order of h_Ω. The ε_p and ε_p' are taken as $(h_\Omega)^2$ and h_Ω.

The theory is validated by the numerical simulation of the collision of two particles. The initial coordinates of the two particles' center are (4, 3) and (8, 3). Two particles went in opposite directions with the initial acceleration of 1. The radius of the particles are 1 (Fig. 11).

The calculated results are shown below (see Fig. 12).

5.2 Particle-wall collisions

The calculation equation for the contact forces F_i^w between particles and wall in the simulation are as bellows

$$F_i^w = \begin{cases} 0 & d_i > 2R_i + \rho \\ \frac{1}{\varepsilon_w}(X_i - X_i')(2R_i - d_i') & 2R_i \le d_i < 2R_i + \rho \\ \frac{1}{\varepsilon_w'}(X_i - X_i')(2R_i + \rho - d_i')^2 & d_i < 2R_i \end{cases} \quad (33)$$

The ε_w and ε_w' are small positive stiffness parameters. In order to study the collision between particles and

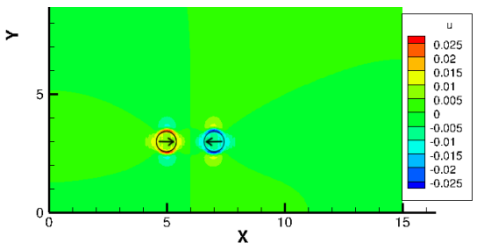

(a) 100 steps

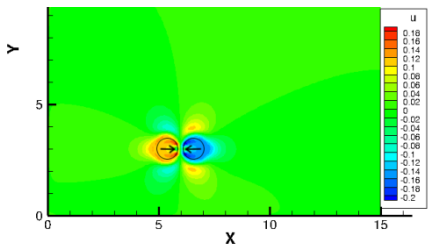

(b) 3000 steps

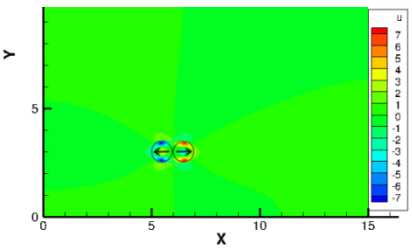

(c) 5700 steps

Fig. 12 The simulation of two particles collision

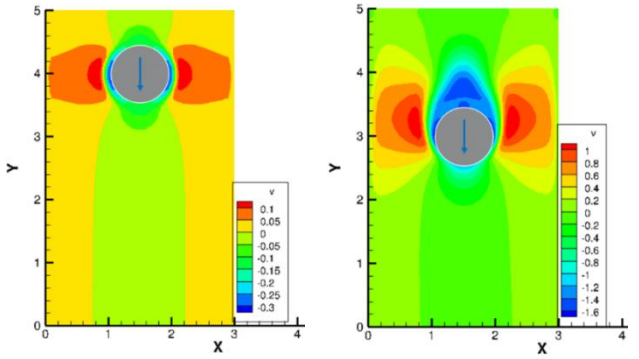

(a) 100 steps (1b) Vortex chart of 1000 steps

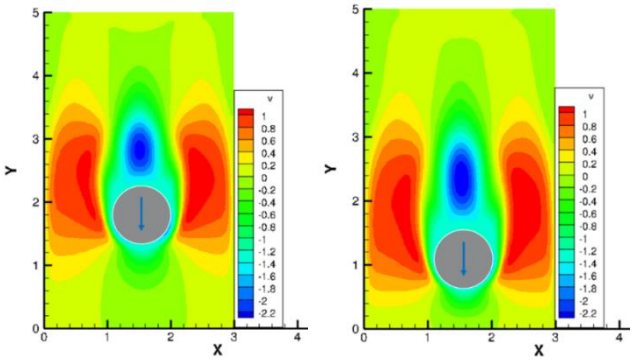

(c) 2000 steps (d) 2500 steps

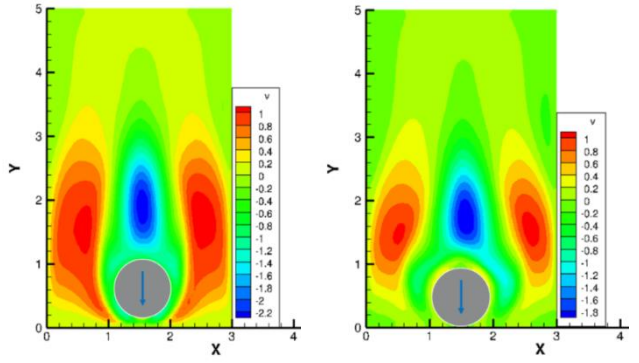

(e) 3000 steps (f) 3500 steps

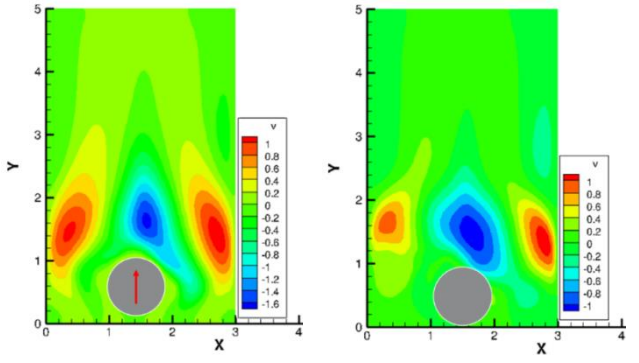

(g) 4000 steps (h) 5000 steps

Fig. 13 Particle-wall collision simulation

boundaries, single particle sediment in the closed fluid area is investigated. The width and length of the domain are 3 and 5. The radius of the particle is 1. The simulation results are shown in Fig. 13. Reynolds numbers is 100 and d_t is 0.001.

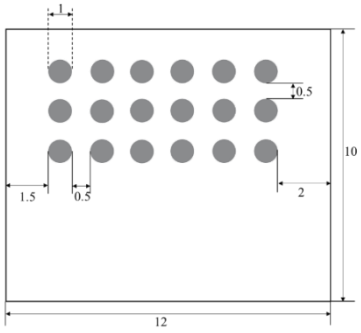

Fig. 14 Schematic diagram of simulation

5.3 The total repulsive force

The total repulsive force of the i particle can be calculated as follows

$$F_i' = \sum_{j=1,j\neq i}^{n} F_{i,j}^{p} + F_i^{w} \tag{34}$$

The trajectories of the particle can be determined by the Newton's motion equation which showed the previous sections and the collision.

For researching convenience, the collision force f_c can be calculated from the normal and tangential direction.

$$f_c = f_n + f_t \tag{35}$$

Where the normal force f_n included the elastic force f_e and the frictional force f_{fm} in normal direction respectively.

$$f_n = f_e + f_{fm} \tag{36}$$

The elastic force was calculated in the equation

In the above sections, the motion of the particles was studied. With the continue motion and the increase in the number of particles, the collisions between particle and wall or particle and particle will take place.

5.4 n particles motion

Based on the interaction between particles and fluid, the collision between the particle-particle and the collision between the particle-wall are studied, the interaction of the large number of the particles and fluids were carried out.

Firstly, the sedimentation of particles were simulated in the closed domain.

The size of the calculation domain is 10×12, a total of 18 particles. The diameter of each particle is 1 and all the particles are divided into three rows at the top of the calculated region (see Fig. 14). Reynolds numbers is 100 and d_t is 0.001. The particles locations and calculation area are shown in Fig. 14.

The interaction between particles and the fluid in the closed domain are shown in Figs. 15-18.

First, the particles are in the top of the area and then begin to sedimentation under the action of gravity. The particle velocity, pressure field and vortex are shown in the following Fig. 15.

As the calculation continues, under the action of gravity,

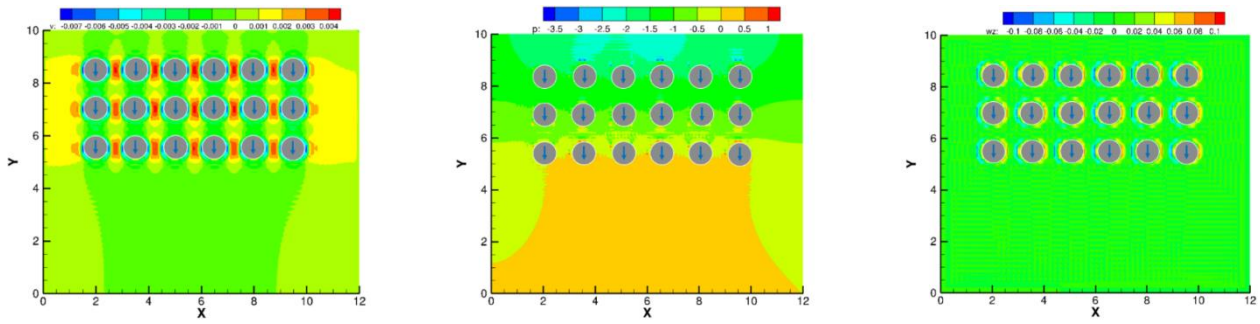

(a) Velocity (b) Pressure field (c) Vortex

Fig. 15 The simulation of particles sedimentation (100 steps)

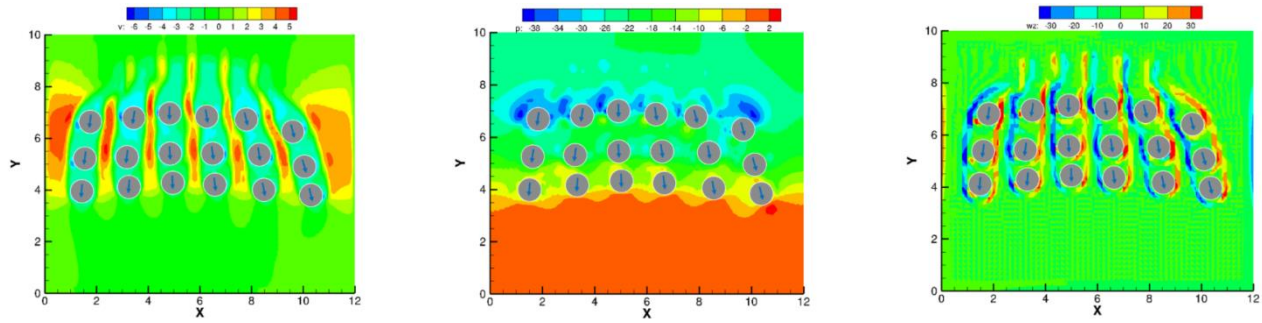

(a) Velocity (b) Pressure field (c) Vortex

Fig. 16 The simulation of particles sedimentation (1000 steps)

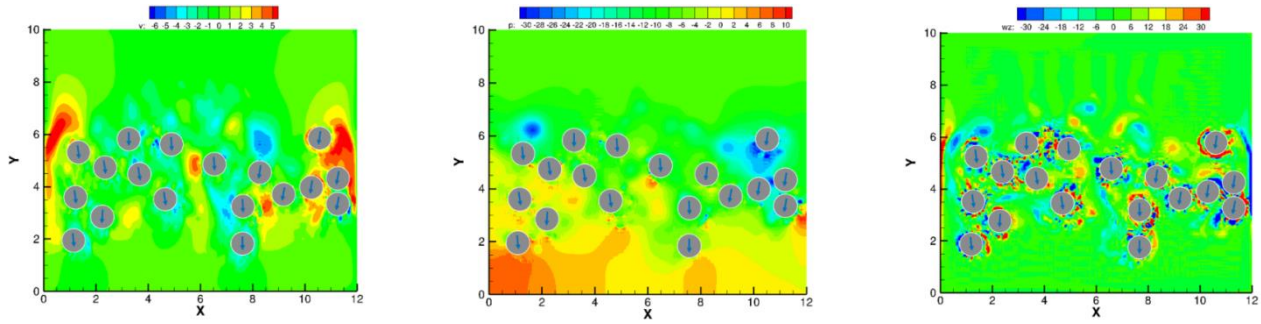

(a) Velocity (b) Pressure field (c) Vortex

Fig. 17 The simulation of particles sedimentation (2000 steps)

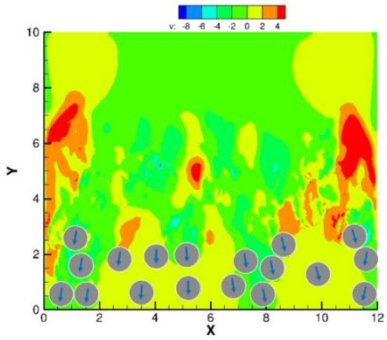

Fig. 18 The simulation of particles sedimentation (3000 steps)

pressure and viscous force, the particles are accelerated to sink and the velocity becomes larger and larger.

From the simulation, we can see that the pressure field has an obvious stratification change for the calculation area which is confined. The pressure field is positive at the bottom of the particles. The pressure field above the particles is negative. With the movement of particles, a large number of vortex generation.

6. Conclusions

(1) In the program, based on the spectral element method and immersed boundary method, the IB-SEM system was established.

(2) By comparing with the previous research on the flow around the cylinder, it is found that the two results are basically the same. The accuracy of the rigid boundary immersion method in the calculation of fluid solid interaction is verified.

(3) The governing equations of motion are established. The migration law of particles under water flow is revealed.

The interaction between particles and fluid is analyzed. The interaction between the lots of particles and the water flow were investigated, which provides a new method for simulating the filling water inrush.

Acknowledgments

The work is supported by the National Natural Science Foundation of China (Grant No. 51679158), Shandong Provincial Natural Science Foundation, China (Grant No. ZR2018BEE045, ZR2017QEE009), China Postdoctoral Science Foundation (2018M630780, 2017T100492, 2017M612273), Fundamental Research Funds of Shandong University (Grant No. 2015GN029).

Reference

Abbas, M., Magaud, P., Gao, Y. and Geoffroy, S. (2014), "Migration of finite sized particles in a laminar square channel flow from low to high Reynolds numbers", *Phys. Fluid.*, **26**(12), 123301.

Colonius, T. and Taira, K. (2008), "A fast immersed boundary method using a nullspace approach and multi-domain far-field boundary conditions", *Comput. Meth. Appl. Mech. Eng.*, **197**(25), 2131-2146.

Hu, H.H., Patankar, N.A. and Zhu, M.Y. (2001), "Direct numerical simulations of fluid-solid systems using the arbitrary Lagrangian-Eulerian technique", *J. Comput. Phys.*, **169**(2), 427-462.

Kumar, B. and Mittal, S. (2012), "On the origin of the secondary vortex street", *J. Fluid Mech.*, **711**(711), 641-666.

Ladd, A.J.C. (1994), "Numerical simulations of particulate suspensions via a discretized Boltzmann equation. Part 1. Theoretical foundation", *J. Fluid Mech.*, **271**(1), 285-309.

Liu, C., Zheng, X. and Sung, C. (1998), "Preconditioned multigrid methods for unsteady incompressible flows", *J. Comput. Phys.*, **139**, 35-57.

Niroumand, H., Mehrizi, M.E.M. and Saaly, M. (2016), "Application of mesh-free smoothed particle hydrodynamics (SPH) for study of soil behavior", *Geomech. Eng.*, **11**(1), 1-39.

Peskin, C.S. (2002), "The immersed boundary method", *Acta Numerica*, **11**, 479-517.

Weirich, D., Köhne, M. and Bothe, D. (2014), "Efficient computation of the flow around single fluid particles using an artificial boundary condition", *Int. J. Numer. Meth. Fluid.*, **75**(3), 184-204.

Williamson, O.E. (1988), "Corporate finance and corporate governance", *J. Finance*, **43**(3), 567-591.

Yang, J. and Stern, F.A. (2015), "A non-iterative direct forcing immersed boundary method for strongly-coupled fluid-solid interactions", *J. Comput. Phys.*, **295**, 779-804.

Zhang, H.Q., Fey, U., Noack, B.R., König, M. and Eckelmann, H. (1995), "On the transition of the cylinder wake", *Phys. Fluid.*, **7**(4), 779-794.

Zhao, T.B., Guo, W.Y., Lu, C.P. and Zhao, G.M. (2016), "Failure characteristics of combined coal-rock with different interfacial angles", *Geomech. Eng.*, **11**(3), 345-359.